Fluid Evolution and Mineralization of Two Distinct High-Sulfidation Epithermal Occurrences in the Toodoggone District, British Columbia, Canada

by

Sinan Canbulat

A thesis submitted in partial fulfillment of the requirements for the degree of

Master of Science

Department of Earth and Atmospheric Sciences
University of Alberta

© Sinan Canbulat, 2023

ABSTRACT

At the Toodoggone District of northern British Columbia, the Ranch area and the Silver Pond zone within the Lawyers area represent two distinct high-sulfidation epithermal occurrences that show some broad similarities but many significant differences. Similarities include some overlaps in terms of gangue mineralogy and alteration style, but pronounced differences include ore mineralogy (relatively simple, comprising few common sulfides at Silver Pond, versus more complex, comprising an array of sulfides and sulfosalts at Ranch) and especially textural styles of mineralization (with common open-space filling textures of veins and breccias at Silver Pond, versus mostly disseminated/replacement style at Ranch with the only open space being sparse vugs). Here, we explore the mineralogy, paragenesis, and fluid evolution of these two nearby yet disparate occurrences to deduce factors that influenced their different styles. Fluid inclusion results clearly indicate persistent boiling throughout the whole paragenesis of both systems. However, microthermometric analyses reveal distinct trends, with evidence of progressive cooling and dilution at Silver Pond, versus apparently isothermal mixing between saline and dilute fluids at Ranch. Specifically, the well-constrained paragenetic sequence of open-space vein minerals at Silver Pond shows a clear and monotonic progression from an early, ~325 °C fluid of ~15 wt.% NaCl eq., towards a later fluid of ~100 °C and nearly zero salinity, consistent with progressive incursion of cold meteoric water. In contrast, the fluids at Ranch show little cooling but span an array of salinities from ~25 wt.% NaCl eq. down to nearly zero, suggesting mixing between a saline magmatic fluid and hot, deeply-circulated groundwater. Hence, these two occurrences seem to represent interesting case studies that document different hydrothermal processes and fluid evolutions, leading to distinct mineralization styles in the epithermal environment.

PREFACE

This thesis is an original work by Sinan Canbulat. No part of this thesis has been previously published.

ACKNOWLEDGMENTS

The successful completion of this thesis is attributed to the invaluable contributions of numerous individuals. First and foremost, my supervisor Matthew Steele-MacInnis to whom I am profoundly grateful for his guidance and unwavering support. Special appreciation is also extended to Pilar Lecumberri-Sanchez for her contributions and tireless efforts. I would like to heartfelt thanks to Sasha Wilson as being a member of the thesis committee as well as Matthew Steele-MacInnis and Pilar Lecumberri-Sanchez, and the staff at APEX Geoscience Ltd, particularly Rob L'Heureux, Rachelle Houge, Emily Laycock, and Edward Parker for their technical guidance, provision of samples, and the imparting of significant information.

Expressly, I am sincerely thankful to my home country, Turkey, and the Ministry of National Education of Turkey for providing me this exceptional opportunity with funding and enabling me to undertake this significant endeavor in this great interval. My gratitude extends to the University of Alberta and all my colleagues for their assistance, including Xinyue Xu and past student Pascal Voegeli.

I dedicate this work to my wife, my parents and all my friends for their unconditional support. A special acknowledgment goes to my wife, whose boundless support, patience, and love have been indispensable to the realization of this work. Without her, this achievement would not have been possible.

TABLE OF CONTENTS

LIST OF TABLES

LIST OF FIGURES

1. Introduction

The Toodoggone district in northern British Columbia, one of the exploration targets for precious metals in Canadian Cordillera, hosts precious metal epithermal and porphyry type deposits such as Baker, Cheni, Shasta, Kemess, Lawyers property, and Ranch project zones. The district mainly consists of Upper Triassic to Lower Jurassic Hazelton Group volcanic and sedimentary rocks, which unconformably overlap submarine island-arc volcanic and sedimentary rocks of the Lower Permian Asitka Group and Middle Triassic Takla Group (Duuring et al., 2009a, 2009b). The Lawyers property, in the area of the historical Cheni mine located in the central region of the Toodoggone district, is an epithermal system that hosts Au-Ag mineralization. While the Lawyers property depicts typical features of a low-sulfidation epithermal system with narrow multiphase quartz-carbonate, quartz-adularia, quartz-sulfide vein, stockwork, and hydrothermal breccia zones, the Silver Pond area within this property exhibits several distinctive characteristics of high-sulfidation style epithermal systems (Duuring et al., 2009a; Voegeli and Lecumberri-Sanchez, 2022). The classification of Silver Pond as a high-sulfidation epithermal system is based on the existence of vuggy quartz with argillic-advanced argillic alteration assemblage (dickite + quartz ± natroalunite + diaspore + topaz) (Bowen, 2014; Diakow et al., 1993, 1991; Duuring et al., 2009a; Voegeli and Lecumberri-Sanchez, 2022). Similarly, the Ranch project zones were similarly classified as high-sulfidation epithermal deposits as they exhibit typical high-sulfidation minerals and alteration assemblages. These zones have gold and subordinate silver and are abundant with Cu-sulfides (chalcopyrite, bornite, covellite, chalcocite) and specifically enargite, a characteristic mineral indicative of high-sulfidation epithermal deposits (Hedenquist, 1995; White and Hedenquist, 1995). The high-sulfidation epithermal systems in the Toodoggone district (e.g., Silver Pond, Ranch Project, Griz-Sickle, Pil South, Nub West) range in age from 200 to 188 Ma,

thus coinciding with the 202 to 197 Ma syenitic porphyry event and the earlier stages of Toodoggone volcanism and suggesting a possible genetic linkage between syenitic-alkalic plutonism, porphyry mineralization, high-sulfidation epithermal mineralization, and volcanism (Duuring et al., 2009b). This magmatic influence has been thought to enhance the ore-forming fluid in terms of favorable acidity and oxidation state, to produce porphyry deposits at depth, with a transition to epithermal deposits, especially high-sulfidation ones, in the shallower portions (Hedenquist and Claveria, 2001). The spatial and genetic relationships from porphyry to epithermal deposits hold significant implications for the exploration of precious metals and ore minerals. Consequently, the Silver Pond and Ranch high-sulfidation epithermal deposits require further investigations to compare in the context of fluid evolution, mineralization, and precious metal content to contribute to the exploration implication in the Toodoggone district, given the strong affinity and transition of epithermal deposits to porphyry type Cu-Au deposits at the deeper part of the surface (Hedenquist et al., 2000; Hedenquist and Claveria, 2001; Sillitoe, 1973).

Here, we present a comprehensive study aimed at elucidating and comparing the mineralizing fluid evolution and mineralization characteristics of the Silver Pond zone (Lawyers Property) and Ranch zones (Bonanza, Thesis, Ridge) high-sulfidation epithermal deposits, particularly with respect to their potential for precious metal enrichment. Additionally, we explore the possible influence on fluids that may be related to alkalic magmatism in the Toodoggone district.

2. Regional Geology

The Toodoggone district, situated in the northern Intermontane Belt of the Canadian Cordillera, is part of the eastern Stikine terrane, which is composed of allochthonous Paleozoic-

Mesozoic calc-alkaline arc complexes and their overlying sedimentary sequences (Monger, 1984). The productive "Golden Horseshoe" trend is formed by several commercial porphyries and epithermal deposits that surround the Middle Jurassic to mid-Cretaceous Bowser Basin and date to the Late Triassic to Early Jurassic in the region. The Toodoggone District, which contains the Ranch and Lawyers properties, comprises Lower Jurassic intermediate volcanic rocks from the Toodoggone Formation, a significant regional member of the Hazelton Group. The Hazelton Group marks the final phase of magmatic arc activity in the Stikine terrane before it accreted onto the Cordilleran Terrane Collage (Gagnon et al., 2012). Latite to dacite volcanic units were deposited in a north-northwest prolonged volcano-tectonic depression of the Toodoggone basement, which contains Lower Triassic Takla Group volcanic rocks and Permian carbonate rocks locally (Diakow et al., 1991). The Jurassic porphyritic plutons known as the Black Lake granitoid intrusive suite intrude the Toodoggone formation and are crosscut by a succession of felsic-intermediate cogenetic dikes (Diakow et al., 1991). The Toodoggone Formation formed concurrently with the establishment of the deep-rooted extensional fault regime, which likely focused on magmatism and controlled the geometric distribution and subsidence of the lithologic units (Diakow et al., 1991). During the Middle to Upper Jurassic depositional hiatus, a massive group of Cretaceous continental sedimentary rocks known as the Sustut Group was deposited, and it defines the youngest unit in the Lawyers property and surrounding region (Diakow et al., 1991). The epithermal deposits hosted in the Toodoggone volcanic rocks are thought to have been preserved by the late sedimentary units during subsequent uplift (Bouzari et al., 2019). The mineral deposits of the Toodoggone district occur in spatial and chronological relationship with one another, usually along similar fault systems and demonstrating associated large-scale mineralogical changes. These deposits display the properties of each end member of the

epithermal-porphyry transition, as represented for example by the porphyry systems of Kemess, Sofia, and Pine, as well as the predominantly low-high sulfidation epithermal systems of Baker, Brenda, Alunite Ridge, Bonanza, Mets, and Lawyers (Fig. 1).

2.1 Mineralization and Alteration

2.1.1 Lawyers (Silver Pond)

Most known deposits on the Lawyers property are hosted within an alteration zone consisting of the assemblage of epidote-chlorite-albite-hematite assemblage, which rarely hosts substantial mineralization. The latest drilling efforts have identified more epidote alteration and an insignificant sericite-smectite component more restricted to deeper stratigraphic sections. The latter is associated with low sulfidation mineralization, which includes significant Au-Ag grades in the form of electrum and native gold, as well as a strong base metal association with Cu, Zn, and Pb in pyrite, chalcopyrite, galena, and sphalerite veins. Within the property, Silver Pond has been classified as a high sulfidation epithermal system since it comprises vuggy quartz with argillic-advanced argillic alteration assemblage (dickite-quartz-natroalunite-diaspore-topaz), as have the Griz-Sickle and Ranch deposit areas (Diakow et al., 1993, 1991; Duuring et al., 2009a; Voegeli, 2022; Voegeli and Lecumberri-Sanchez, 2022).

At the proximal Baker Mine, molybdenite Re-Os dating revealed an age of 193.8 ± 0.8 Ma (Bouzari et al., 2019). These Re-Os molybdenite dates from also Baker match Pb^{206}-U^{238} crystallization dates from Duncan Pluton of the Black Lake Intrusive suite (oldest age of 202.3 ± 2.3 Ma and youngest date of 193.4 ± 2.6 Ma). The ages of intrusions and mineralization in the Toodoggone District most likely imply multiple pulses of magmatism. Many weakly altered dikes that crosscut Albert's Hump, located to the north of the Lawyers Property, and Silver Pond, are

similar in composition and texture to the dikes that crosscut the intrusions of the Black Lake Suite and thus are concurrent or post-date the earliest date (~193-190 Ma) of cooling of the intrusive.

2.1.2 Ranch

The Ranch property is characterized by high-sulfidation (acid-sulfate) epithermal alteration, defined by widespread argillization and silicification of andesite-dacite host rocks. In a typical zonal epithermal alteration system, assemblages include alunite-quartz, hematite-illite-quartz, dickite-quartz, quartz-baryte, and quartz-pyrite (Bowen, 2014). The primary mineralization includes argentite, electrum, native gold, and silver, as well as chalcopyrite, galena, and sphalerite. Porphyry-style mineralization is also prevalent in the surrounding areas but has yet to be intersected on the property itself. All significant gold mineralization on the Ranch property is hosted by silica-sulfate and silica-sulfide bodies surrounded by argillic-altered zones (Bowen, 2014). The primary alteration assemblage directly next to auriferous zones is dickite-quartz, which generally contains anomalous levels of gold, accompanied locally by anomalous concentrations of zinc, lead, or copper. Economic gold grades are almost always found in alteration assemblages containing quartz-baryte-pyrite ± copper sulfides, quartz-pyrite ± copper sulfides, or, in rare cases, copper-lead-zinc sulfides (Bowen, 2014).

The BV, Thesis, and Bonanza zones are the three mineralization zones on the Ranch property that have featured small-scale previous production. Gold mineralization is hosted by a quartz-baryte-pyrite-sericite assemblage at the BV zone, a quartz-baryte-pyrite (chalcopyrite, galena, sphalerite) assemblage at Thesis, and a quartz-baryte and quartz-pyrite-chalcopyrite-enargite-bornite-(baryte) assemblage at Bonanza. At the Ridge Zone, the significant assemblage has been recognized as quartz-hematite-pyrite in the ore veins (Bowen, 2014).

3. Samples and Methods

Polished thin sections from the Silver Pond and Ranch zones (Bonanza, Thesis, Ridge) were prepared for preliminary petrographic studies and investigated by optical and reflected light microscopy. Then, suitable thin sections were selected for further investigations through microthermometry, SEM-EDS analyses and Raman spectroscopy. Reflected light microscopy was used to determine ore minerals disseminated in the host rock. Optical polarized-light microscopy was employed for investigating vein mineralogy, textures, and cross-cutting relationships to produce relative paragenesis sequences for both distinct deposits. Additionally, fluid inclusion petrography, including size, shape, spatial relationships, phases, and phase ratios, was determined based on the criteria of (Bodnar et al., 1985; Goldstein and Reynolds, 1994; Nash, 1976; Roedder, 1984).

Scanning electron microscopy (SEM) integrated energy dispersive spectroscopy (EDS) analyses were performed by Zeiss Sigma 300 VP-FESEM in the University of Alberta, Earth and Atmospheric Science. All analyses were done under low vacuum (VP Mode) since samples were not carbon-coated, along an accelerating voltage of 25 kV, while the detector distance was 5-10 mm above the specimen.

Microthermometric measurements were conducted on 90 fluid inclusions of primary, secondary, and uncertain origin. forty-eight belong to Ranch zones, and forty-two are in the Silver Pond. Quartz, calcite, baryte, and anhydrite are host minerals in the Silver Pond, while quartz and baryte were the hosts in Ranch samples. Measurements were performed at the University of Alberta, Earth, and Atmospheric Sciences, using Linkam THMS600 freezing-heating stage calibrated using known temperature transitions of synthetic fluid inclusions, combined with a custom-built Olympus BX-series petrographic microscope. Accuracy and precision of the

temperature measurements was ± 1 ºC and ± 0.1 ºC for heating and freezing, respectively. Salinity (wt.% NaCl) and homogenization temperature were calculated by HokieFlincs (Steele-MacInnis et al., 2012).

4. Results

4.1 Paragenesis

4.1.1 Mineralization

Based on optical and reflected light microscopy investigations, sulfide minerals are mainly hosted in the altered volcanic host rock as disseminated grains in the Silver Pond (Fig. 2a). Isometric (cubical) pyrites (FeS_2) are the main sulfide minerals in disseminated zones in the Silver Pond (Fig. 2b, d, e, f). However, a significant proportion of the pyrite was partly replaced by chalcopyrite as a supergene occurrence (Fig. 2d, e, f). The majority of the sulfide mineralization was hosted in the wall rock and was generally not observed in the veins or veinlets as a stockwork or breccia body in the Silver Pond, with the exception of sphalerite that was fairly common within the veins. Rarely, pyrite was observed in the anhydrite veins or breccias (Fig. 2c). As a result of this general separation of sulfides from the veins, the paragenetic relationship between sulfide minerals (other than sphalerite) and hydrothermal gangue minerals was for the most part unclear.

All Ranch samples from Bonanza, Thesis, and Ridge zones contain sulfide minerals as well as discrete gold grains, distributed mainly as disseminated grains and less commonly as veinlets within the altered volcanic host rock (Fig. 3a, b, c, e, h). The hypogene occurrences of gold grains, chalcopyrite, and pyrite minerals are evident (Fig 3a, b, e, h), whereas Cu-sulfides (bornite-covellite-chalcocite) suggest supergene origins on chalcopyrite grains (Fig. 3c, d, f). Additionally, euhedral to subhedral magnetite grains are commonly disseminated in the volcanic host rock (Fig.

3g), and lesser enargite was detected in cavities of sulfide minerals. Again, we found no clear evidence of the paragenetic relationship between sulfide mineralization or gold grains with gangue minerals in the veins or disseminated grains.

Seven principal gangue minerals within veins and veinlets were identified via optical microscopy observations in the Silver Pond zone. The distinguished mineral assemblage comprises quartz with a number of textural types (feathery, euhedral, microcrystalline), sphalerite, calcite, and sulfate minerals (anhydrite and baryte) (Fig. 4). Three prominent vein types were distinguished: 1) QSpC veins, including ± quartz (feathery+euhedral), + sphalerite, ± calcite; 2) Solo-sulfate veins (SS) composed of monomineralic anhydrite, which did not show any clear relation with the other veins owing to a lack of cross-cutting relationships; and 3) Sulfate-bearing veins consisting of baryte, quartz (feathery ± euhedral ± microcrystalline), ± calcite. Additionally, coarse colorless fluorite grains occurred in a fourth vein type that was observed only in two samples. However, the latter veins did not exhibit any clear relationship with gangue minerals in the other vein assemblages. Some of the main features of each of the principal vein minerals at Silver Pond are outlined next.

Quartz—Three distinct textural types of quartz were identified, namely feathery quartz, euhedral quartz, and microcrystalline quartz (Fig. 4a, b, d). Feathery and euhedral quartz were both generally correlated with sphalerite in the veins (Fig. 4a, b), whereas microcrystalline quartz veinlets did not show any relationship with sphalerite. Note that feathery quartz is generally considered to provide evidence of fluid boiling in epithermal environments (Moncada et al., 2012).

Sphalerite—Euhedral to anhedral greenish-colored sphalerite crystals were unique amongst the sulfides as being the only type of sulfide mineral found routinely within the veins. Sphalerite

crystals are generally encompassed by quartz (euhedral and feathery) (Fig. 4a, b), and they generally surround the calcite crystals in the veins and veinlets (Fig. 4a, c).

Calcite—Calcite grains are included as large crystals by several veins (Fig. 4a, c). Rhombic calcite crystals, thought to reflect slow-growth during non-boiling conditions (Moncada et al., 2012), are common at Silver Pond (Fig. 4a). According to textural and cross-cutting relationships, calcite crystals precipitated after feathery-euhedral quartz and sphalerite mineralizations but before microcrystalline quartz (Fig 4a, b, c, d).

Sulfate Minerals—Abundant tabular baryte crystals are in the veins closely associated with microcrystalline quartz. Also, quartz occurrences (feathery±euhedral) are located in the wall boundary of baryte (Fig. 4e). In contrast, microcrystalline quartz can be seen as either a distinct vein cutting baryte minerals or coexisting in the same zone through baryte minerals. Thus, baryte formations represent not only the middle stage but also indicate the latest stage of mineralization with microcrystalline quartz. Also note that baryte commonly hosted inclusions of pyrite grains (Section 4.2), indicating that baryte postdated at least some of the pyrite. Anhydrite crystals are commonly seen as single minerals in the veinlets (Fig. 4f). In thin, monomineralic anhydrite veinlets, no evident relationship with the other veins/veinlets was observed.

The relative mineral paragenetic sequence showing two related distinct veins (QSpC and Sulfate-bearing) was produced according to mineralogy, texture, and cross-cutting relationship regarding the Silver Pond epithermal deposit. (Fig. 5).

Ranch samples have two transparent minerals as gangue in the host rock. Vug-filling quartz and independent baryte crystals (tabular or acicular) can be found without any clear relationship

with one another nor with the sulfide minerals (Fig. 6a, b, d, e, f.). Few primary (igneous) quartz phenocrysts are present in the volcanic host rock as well (Fig. 6c).

4.2 SEM-EDS Results

At Silver Pond, the main sulfide minerals are pyrite (FeS_2) (Fig. 7a-a, b, c) and subordinate sphalerite (ZnS), galena (PbS) with chalcopyrite ($CuFeS_2$). Cubic pyrites included within baryte grains were detected by the SEM, which reinforces the interpretation of a relatively high sulfidation state of the Silver Pond (Fig. 7a-a). Based on EDS results, the Silver Pond area showed less evidence for free-milling gold, compared to the Ranch zones with a more complex sulfide assemblage and obvious free-milling Au. Lastly, an uncommon occurrence of baryte crystals, included by anhydrite grain, was recorded (Fig. 7a-d). Hence, even though we did not observe a conspicuous petrographical relationship between baryte and anhydrite under the polarized microscope at Silver Pond, this one observation suggests that the anhydrite veinlets may be relatively late in the paragenetic sequence.

Pure gold grains have been detected in Ranch samples under SEM (Fig. 7b-a, b, d). Cu-sulfide minerals, including bornite, chalcocite, covellite, and chalcopyrite, can be found in mainly Ridge zone samples, and they do not show any obvious relationship with gold grains in the mineralized zones. In some cases, baryte crystals showed a close spatial relationship with gold grains as a vug filling (Fig. 7b-b). Additionally, EDS analyses revealed some occurrence of Te-tetrahedrite subgroup minerals consisting of Cu-Sb-Te-S, bismuthian tetrahedrite (Cu-Fe-Zn-Bi-Sb-As-bearing) on the edge of sulfide minerals over backscattered electron (BSE) imaging (Fig. 7b-c).

4.3 Fluid Inclusion Studies by Paragenesis Stages

Fluid inclusion petrography and microthermometry were applied to gain consistent data about fluid properties with the criteria of (Bodnar et al., 1985; Goldstein and Reynolds, 1994; Nash, 1976; Roedder, 1984). We analyzed inclusions in quartz, baryte, calcite and anhydrite. Inclusions in sphalerite were unfortunately too dark (nearly opaque) to be workable. We also tested the pyrites by infrared (IR) light microscopy, but all pyrites in the Silver Pond and Ranch samples were found to be opaque in IR. We also tested inclusions in all samples by Raman spectroscopy, but found no detectable signals in either Silver Pond or the Ranch zones.

4.3.1 Fluid Inclusion Petrography

Silver Pond

Feathery and microcrystalline quartz minerals were unsuitable for investigating fluid inclusion properties due to their small grain sizes. Euhedral quartz grains, however, generally contained clearly primary fluid inclusions in the growth zones, which mainly consisted of aqueous vapor-rich and lesser aqueous liquid-rich inclusions in the size of 5 to 10 μm (Fig. 8a, b). They mostly contained ~80 to 100% vapor phase by volume as a single phase. Solely aqueous vapor-rich fluid inclusions in the same fluid inclusion assemblage (FIA) is generally considered an indicator of flashing/boiling (Bodnar et al., 2014; Steele-MacInnis, 2018).

Calcite crystals mainly hosted secondary or uncertain-origin fluid inclusions inside healed fractures. Sizes of fluid inclusions vary between 5 to 10 μm (Fig. 8c, d). Both aqueous liquid- and vapor-rich fluid inclusions populations comprise the whole population. Aqueous liquid-rich two-phase inclusions contain up to >80 % liquid by volume, while aqueous vapor-rich inclusions comprise up to 100% vapor phase. Concurrence of aqueous liquid- and vapor-rich fluid inclusions

in the same FIA is an indicator of fluid boiling (Bodnar et al., 1985; Haas, 1971; Moncada et al., 2012).

Baryte crystals mainly involve secondary or uncertain origin fluid inclusions, commonly aqueous vapor-rich and lesser aqueous liquid-rich, ranging from 5 to 10 μm (Fig. 8e, f). Aqueous vapor-rich fluid inclusions compose the entire population, including up to 100 % vapor phase.

Anhydrite minerals commonly have secondary and uncertain origin fluid inclusions in fractures and cleavages, mainly aqueous vapor-rich and lesser liquid-rich. The shapes of fluid inclusions show a negative or irregular distribution with a size of up to 10 μm (Fig. 8g, h). Vapor-rich inclusions, in most cases, contain up to 100% vapor phase in volume.

Ranch Project (Bonanza, Thesis, Ridge)

Primary quartz phenocrystals contain secondary fluid inclusions assemblages cutting primary vapor-rich fluid inclusions in Bonanza zone (Fig. 9a, b). Aqueous liquid-rich fluid inclusions are abundant in this zone, ranging between 5 to 10 μm. Some visually include 40% vapor phase by volume; however, the liquid phase mainly consists of up to 80% of the total phase volume (Fig. 9b).

Baryte is the most abundant host mineral for fluid inclusions in Ranch zones. The origin of the fluid inclusions remains uncertain due to the lack of clear primary or secondary features (Fig. 9c). The size of the inclusions is generally around 5 to 10 μm. Both aqueous liquid- and vapor-rich fluid inclusions populations comprise the whole population. Aqueous liquid-rich two-phase inclusions contain up to >70 % liquid by volume, while aqueous vapor-rich inclusions consist of up to 100% vapor phase (Fig. 9e, f). Again, the coexistence of aqueous liquid- and vapor-rich fluid

inclusions in the same FIA provides evidence for fluid boiling (Fig. 9d) (Bodnar et al., 1985; Haas, 1971; Moncada et al., 2012).

4.3.2 Microthermometry

The measured average homogenization temperature of primary fluid inclusions in euhedral quartz of Silver Pond deposit is 321 °C, while uncertain origin fluid inclusions of calcite, baryte, and anhydrite are 291 °C, 211 °C, and 158 °C, respectively. The average salinity of primary fluid inclusions, based on measured ice-melting temperatures, in euhedral quartz was evaluated at 13.4 wt.% NaCl equivalent (eq.), and the uncertain origin fluid inclusion of calcite, baryte, and anhydrite yielded average salinities of 10.3 wt.% NaCl eq., 9.5 wt.% NaCl eq., and 1.0 wt.% NaCl eq., respectively. A detailed summary of microthermometry results for both the Silver Pond and Ranch zones can be found in Table 1.

Table 1: Microthermometry Results

Region	Zone	Inclusion type	Host mineral	Inclusion origin	Tm_{ice}/°C	Th/°C	Salinity (wt. % NaCl eq.)
Lawyers	Silver Pond	L+V	Euhedral quartz	Primary (11)	-7.4 to -11.4	307-349	11.0-15.3
		L+V	Calcite	Uncertain (8)	-4.5 to -8.3	285-297	7.3-11.8
		L+V	Baryte	Uncertain (10)	-3.1 to -9.6	75-329	5.1-13.5
		L+V	Anhydrite	Uncertain (9)	-0.3 to -1.1	86-177	0.4-1.9
Ranch	Bonanza	L+V	Quartz	Secondary (8)	-2.9 to -4.9	202-235	4.8-7.7
		L+V	Baryte	Uncertain (8)	-3.5 to -8.2	191-230	5.7-11.9
	Ridge 143.4	L+V	Baryte	Uncertain (9)	-0.6 to -1.7	216-320	0.5-2.4
	Ridge 154.5	L+V	Baryte (FIA1)	Uncertain (10)	-3.8 to -9.2	222-280	6.2-13.1
	Ridge 154.5	L+V	Baryte (FIA2)	Uncertain (12)	-9.1 to -22.4	301-326	13.0-24.0

The Ranch zones showed distinct homogenization temperatures and salinities. Secondary fluid inclusions in quartz in Bonanza zone showed homogenization temperature of 212 °C and salinity of 6.1% wt. NaCl equivalent. Uncertain origin fluid inclusions in baryte at Bonanza zone showed homogenization temperature of 206 °C, and salinity of 9.1 wt.% NaCl eq.. Regarding Ridge zone

barytes, homogenization and ice melting temperatures of fluid inclusions exhibit different distributions with decreasing depth, from 154.5 to 143.4 m. Homogenization temperatures shifted from 318 °C to 247 °C, over this depth interval, while salinity varied from 13.7 wt.% to 1.7 wt.% NaCl eq. on average. Some of the vapor inclusions showed melting at -60 °C, to -70 °C, suggesting a small amount of $CO_2 \pm CH_4$ in the fluid.

Homogenization temperature (*Th*) ranges versus salinity (wt.% NaCl eq.) plot was produced to reveal the complex sequence of fluid evolution processes and characteristics of hydrothermal systems for the Silver Pond and Ranch zones (Fig. 10a, b). On top of the considerable evidence for fluid boiling throughout the paragenesis at both Silver Pond and Ranch zones, the results show also that fluid mixing and cooling also took place and probably influenced the mineralization. The salinity distributions of fluid inclusions in these two deposits are consistent with fluid from a magmatic source, mixing with a lower-salinity ambient fluid. Decrease in salinity accompanied by decreasing *Th* is the main trend at Silver Pond (Fig. 10a), suggesting that the hot magmatic fluid mixed with a cold, surface-derived (meteoric) water. In contrast, fluids from the Ranch zones show similar changes in salinities within a much more limited range of homogenization temperatures, suggesting isothermal fluid mixing between a saline and a dilute fluid that were both at similar temperatures (Fig. 10b). We suggest that it is likely that the magmatic fluid at the Ranch zone mixed with dilute surface-derived water that had first circulated more deeply and acquired higher temperature prior to mixing.

5. Discussion

5.1 Similarities and Differences in Terms of Mineral Assemblages and Texture

Gangue minerals in the Silver Pond and Ranch project zones show some similarities and some differences. Both zones contain tabular and acicular baryte minerals, along with quartz. However, the Silver Pond zone has distinct textural features in its quartz minerals, such as feathery, euhedral, and microcrystalline, coexisting with calcite and a lesser sphalerite within open-space filling veins or veinlets. Anhydrite veins demonstrate separate distribution in the host rock as thin solo-sulfate veinlets in the Silver Pond. In contrast, the Ranch zones exclusively exhibit isolated quartz filling vugs within the host rock, lacking any apparent indications of baryte mineralization associated with veins. The relative mineral paragenetic sequence is discernible in the Silver Pond zone, owing to observations of vein mineralogy, cross-cutting relationships, and textural features (Fig. 4). The presence of feathery quartz in this zone suggests the potential occurrence of a boiling phenomenon during mineralization. This inference is rooted in the fluid boiling textures, which are linked to rapid mineral deposition, although the presence of rhombic calcite within the same vein suggests non-boiling conditions, according to prior studies (Dong et al., 1995; Moncada et al., 2012; Sander and Black, 1988). The interpretation of the conditions prevailing during mineralization in the Ranch zones is challenging due to the general dearth of veins. These zones exclusively consist of isolated vug fillings, encompassing either quartz or baryte minerals, rendering it unfeasible to determine the predominant conditions via relative mineral paragenetic sequence.

The sulfide minerals and precious metals of the Silver Pond zone and Ranch project zones again show notably differences from each other based on our reflected light microscopy and SEM-EDS observations. Silver Pond primarily hosts disseminated pyrite, subordinate chalcopyrite,

galena, and sphalerite as sulfide minerals. Meanwhile, the Ranch zones are enriched with pyrites and supergene Cu-sulfides (bornite, covellite, chalcocite) on chalcopyrite and pyrite, especially in Ridge zone. In contrast, Bonanza and Thesis zones host abundant electrum Au grains with trace Ag, enargite (Cu_3AsS_4), and tetrahedrite subgroup minerals, including Sb, Te, and Bi. Neither the Silver Pond nor Ranch zones show much evidence of sulfide minerals in veins, with the main exception being sphalerite in veins at Silver Pond. Instead, the sulfides are predominantly encountered as disseminated grains or massive aggregates in the altered wall rock.

5.2 Sulfidation State

Both the Silver Pond and Ranch zones bear hallmarks of high sulfidation epithermal deposit based on our findings and in light of previous studies. High sulfidation and low sulfidation epithermal deposits have some characteristic differences in the sense of gangue and ore mineralogy and form of deposit as well as alteration assemblages (Arribas, 1995; Barton, 1981; Hedenquist et al., 2000; Richards, 2013; Sillitoe and Hedenquist, 2003; White and Hedenquist, 1995). Disseminated and replacement ore forming without any veins or veinlets, including sulfide and sulfate minerals together, the occurrence of enargite and tetrahedrite subgroup minerals are some key indicators of high sulfidation epithermal deposits, along with argillic and advanced argillic alteration assemblages consisting of clay minerals such as kaolinite, dickite, and alunite. The Silver Pond and Ranch project zones reflect nearly identical deposit forms, including disseminated sulfide minerals in the host rock. However, the gangue minerals of the Silver Pond zone mainly occur in the veins or veinlets, which is different from Ranch zones. Sulfides, mainly pyrite, chalcopyrite, and sulfate minerals, mostly baryte, can be seen in these two distinct epithermal deposits, and the co-occurrence of pyrite as inclusions in baryte provides additional evidence that these minerals were in equilibrium. The sulfide mineral assemblage of the Silver Pond, mainly

consisting of pyrite, sphalerite, chalcopyrite, and galena, reflects some elements that appear transitional state towards intermediate to low sulfidation (Wang et al., 2019). However, the Silver Pond zone also includes kaolinite, dickite, and alunite clay minerals of argillic alteration products, which are strong evidence of high sulfidation epithermal deposits (Diakow et al., 1993, 1991; Duuring et al., 2009a; Voegeli, 2022; Voegeli and Lecumberri-Sanchez, 2022).

Ranch zones have been reported as consisting of enargite and Te- Bi-bearing tetrahedrite minerals, confirmation of high sulfidation epithermal deposit with argillic/advanced argillic alteration mineralogy, which is another unambiguous evidence of high-sulfidation epithermal deposits (Bowen, 2014; White and Hedenquist, 1995).

5.3 Fluid Evolution

The Silver Pond and Ranch deposits both exhibit signs of boiling, including the presence of liquid and vapor-rich inclusions within the same assemblages and boiling indicator mineral textures like feathery quartz (Bodnar et al., 2014, 1985; Chen et al., 2022; Haas, 1971; Moncada et al., 2012; Steele-MacInnis, 2018). However, microthermometric results of fluid inclusions reveal unique characteristics of the fluid evolution and deposit properties. The Silver Pond deposit shows a clear cooling pattern along with progressive dilution, suggesting a mixing of magmatic-hydrothermal fluid with cold meteoric water. That is supported by the homogenization temperatures and salinity results, which overlap with the relative mineral paragenesis sequence stages. As previously observed by (Canet et al., 2011; Cooke and Bloom, 1990; Hedenquist and Henley, 1985; Liu et al., 2019; Mehrabi et al., 2016; Wilkinson, 2001), during mineralization, isothermal mixing is recognized from quartz to calcite, with similar salinity values ranging from 10-15% wt. NaCl eq. and slightly decreasing homogenization temperatures from 350 to 300 °C in (Fig. 10a). The cooling pattern then shifts to dilution from calcite to anhydrite, with a sharp decline

in homogenization temperature and salinity, from 300 to 100 °C and approximately 12 to 0.3% wt. NaCl eq., respectively.

Microthermometry analyses of the Ranch zones, particularly the Ridge zone, indicate the presence of saline and heated fluids (Fig. 10b). These zones exhibit a complex pattern of high-temperature fluid properties with fluctuating salinity values ranging from 0.5 to 24% wt. NaCl eq. The homogenization temperatures of the fluid range between 250-320 °C, with a minimum of 191 °C during cooling and mixing. The fluid in the Ranch zones might have originated from the mixing of magmatic-hydrothermal fluid with deeply circulated and heated meteoric water, which was hotter than that at Silver Pond.

5.4 Potential Contributions of Alkalic Magmatism in the Silver Pond and Ranch Zones

So far, definitive evidence for the magmatic fluid source is mostly lacking, and the question of whether these deposits relate to an alkalic magmatic contribution remains open. However, the presence of Bi- and Te-bearing tetrahedrite subgroup minerals on sulfide minerals could indicate alkalic magmatism in the Ranch zones (Fig. 7b-c). This phenomenon is especially relevant considering that Te-bearing gold and silver minerals and enrichment of Te anomalies are commonly associated with alkalic magmatic origins of epithermal deposits (Kelley and Ludington, 2002). Researchers have jointly reported the presence of Te (Telluride), Se (Selenide), and Tl (Thallium) as trace minerals associated with gold in metallogenic belts and areas of alkalic magmatism (Ciobanu et al., 2006; Jensen and Barton, 2000; Spooner, 1993). Silver Pond contains at least Se (up to 24,000 ppm) and Tl (up to 1,200 ppm) based on depth via drill core samples (Voegeli and Lecumberri-Sanchez, 2022). Fluorite mineralization, too, is widely considered as evidence of epithermal mineralization related to alkalic magmatism (Gagnon et al., 2003). Rare but unambiguous hydrothermal fluorite found in the Silver Pond samples may thus also suggest a

contribution of alkalic magmatism in this deposit. Besides, the abundance of alkalic porphyry Au-Cu deposits in western British Columbia, such as Galore Creek, Kerr, Sulphurets, Mount Polley, Red Chris, Lorraine, Copper Mountain, Afton, and Mount Milligan (Barr et al., 1976; Lang et al., 1995; Thompson et al., 2001), points out the importance of alkalic magmatism this overall region.

6. Conclusion

1) Both the Silver Pond and Ranch zones show clear boiling evidence in terms of fluid inclusion petrography and mineral textures. Microthermometric results also point to cooling patterns of these two distinct epithermal deposits. Ranch and the Silver Pond exhibit cooling by probable mixing of magmatic-hydrothermal fluid with meteoric water. However, at Ranch this mixing took place more or less isothermally, suggesting that the meteoric end-member was deeply-circulated and heated. In contrast, the mixing fluid at Silver Pond fluid was cold meteoric water.

2) The Ranch zones exhibit noticeable amount of evidence for the presence of various sulfide minerals with free-milling gold, including electrum gold (Au-Ag alloy) with trace amounts of Ag, supergene Cu-sulfides (bornite, chalcocite, covellite) on chalcopyrite and pyrite, as well as sparse enargite and Sb-Te-Bi-bearing tetrahedrite subgroup minerals; as compared to a much simpler sulfide mineralogy at Silver Pond. The dissimilarity in mineralogy and free-milling Au content between the Ranch zones and the Silver Pond can probably be attributed to the differences in fluid evolution characteristics.

3) The Ranch and Silver Pond deposits demonstrate significant characteristics of high sulfidation epithermal systems in the context of mineralogy associations, deposit forms, and alteration assemblages. These characteristics include argillic/advanced argillic alteration haloes that involve clay minerals such as dickite, kaolinite, and alunite, as well as mineral associations

(coeval sulfides and sulfates). Moreover, identifying enargite, Te- and Bi-bearing tetrahedrite minerals on Cu-sulfides provides convincing evidence of a high sulfidation system in Ranch zones.

4) The potential influence of alkalic magmatism on these two high-sulfidation epithermal deposits should be considered, given the occurrence of fluorite and Te- and Bi-bearing tetrahedrite subgroup minerals and anomalies. The broad distribution of alkalic Au-Cu porphyries in western British Columbia reinforces the probable alkalic hypothesis, but more study is required to address this conclusively.

References

Arribas, A., 1995. Characteristics of high-sulfidation epithermal deposits, and their relation to magmatic fluid. Mineral. Asso. Canada Short Course Series 23.

Barr, D.A., Fox, P.E., Northcote, K.E., Preto, V.A., 1976. The alkaline suite porphyry deposits: A summary. Porphyry Deposits of the Canadian Cordillera, Sutherland Brown, A., Editor, Canadian Institute of Mining and Metallurgy, Special 15, 359–367.

Barton, P.B., 1981. Physical-chemical conditions of ore deposition. Physics and Chemistry of the Earth 13–14, 509–528. https://doi.org/10.1016/0079-1946(81)90024-0

Bodnar, R., Lecumberri-Sanchez, P., Moncada, D., M., S.-M., 2014. Fluid Inclusions in Hydrothermal Ore Deposits, in: Treatise on Geochemistry: Second Edition. pp. 119–142. https://doi.org/10.1016/B978-0-08-095975-7.01105-0

Bodnar, R., Reynolds, T.J., Kuehn, C.A., 1985. Fluid inclusion systematics in epithermal systems, in Berger, B.R., and Bethke, P.M., eds., Geology and Geochemistry of Epithermal Systems. Reviews in Economic Geology 2, 73–97.

Bouzari, F., Bissig, T., Hart, C.J.R., Leal-Mejia, H., 2019. An Exploration Framework for Porphyry to Epithermal Transitions in the Toodoggone Mineral District (94E) (No. MDRU Publication 424).

Bowen, B.K. (Barney), 2014. Technical Report On the Ranch Project Liard mining division British Columbia, Canada.

Canet, C., Franco, S.I., Prol-Ledesma, R.M., González-Partida, E., Villanueva-Estrada, R.E., 2011. A model of boiling for fluid inclusion studies: Application to the Bolaños Ag–Au–

Pb–Zn epithermal deposit, Western Mexico. Journal of Geochemical Exploration 110, 118–125. https://doi.org/10.1016/j.gexplo.2011.04.005

Chen, X., Zhou, Z., Chen, Y., Barrier, J., Steele-MacInnis, M., 2022. Fluid boiling during high-grade gold deposition in an epithermal gold-telluride deposit, Guilaizhuang, China. Journal of Geochemical Exploration 240, 107048. https://doi.org/10.1016/j.gexplo.2022.107048

Ciobanu, C., Cook, N., Spry, P., 2006. Preface – Special Issue: Telluride and selenide minerals in gold deposits – how and why? Mineralogy and Petrology 87, 163–169. https://doi.org/10.1007/s00710-006-0133-9

Cooke, D.R., Bloom, M.S., 1990. Epithermal and subjacent porphyry mineralization, Acupan, Baguio District, Philippines: a fluid-inclusion and paragenetic study. Journal of Geochemical Exploration 35, 297–340. https://doi.org/10.1016/0375-6742(90)90042-9

Diakow, L.J., Panteleyev, A., Schroeter, T.G., 1993. Geology of the Early Jurassic Toodoggone Formation and gold-silver deposits in the Toodoggone River map area, northern British Columbia, Bulletin (British Columbia. Ministry of Energy, Mines and Petroleum Resources). Ministry of Energy, Mines and Petroleum Resources, Victoria, B.C.

Diakow, L.J., Panteleyev, A., Schroeter, T.G., 1991. Jurassic epithermal deposits in the Toodoggone River area, northern British Columbia; examples of well-preserved, volcanic-hosted, precious metal mineralization. Economic Geology 86, 529–554. https://doi.org/10.2113/gsecongeo.86.3.529

Dong, G., Morrison, G., Jaireth, S., 1995. Quartz textures in epithermal veins, Queensland - classification, origin, and implication. Economic Geology 90, 1841–1856. https://doi.org/10.2113/gsecongeo.90.6.1841

Duuring, P., Rowins, S., McKinley, B., Dickinson, J., Diakow, L., Kim, Y.-S., Creaser, R., 2009a. Examining potential genetic links between Jurassic porphyry Cu–Au ± Mo and epithermal Au ± Ag mineralization in the Toodoggone district of North-Central British Columbia, Canada. Mineralium Deposita 44, 463–496. https://doi.org/10.1007/s00126-008-0228-9

Duuring, P., Rowins, S.M., McKinley, B.S.M., Dickinson, J.M., Diakow, L.J., Kim, Y.-S., Creaser, R.A., 2009b. Magmatic and structural controls on porphyry-style Cu–Au–Mo mineralization at Kemess South, Toodoggone District of British Columbia, Canada. Miner Deposita 44, 435–462. https://doi.org/10.1007/s00126-008-0227-x

Gagnon, J., Barresi, T., Waldron, J., Nelson, J., Poulton, T., Cordey, F., 2012. Stratigraphy of the upper Hazelton Group and the Jurassic evolution of the Stikine terrane, British Columbia. Canadian Journal of Earth Sciences 49, 1027–1052. https://doi.org/10.1139/e2012-042

Gagnon, J.E., Samson, I.M., Fryer, B.J., Williams-Jones, A.E., 2003. Compositional Heterogeneity in Fluorite and The Genesis of Fluorite Deposits: Insights From LA–ICP–MS Analysis. The Canadian Mineralogist 41, 365–382. https://doi.org/10.2113/gscanmin.41.2.365

Goldstein, R.H., Reynolds, T.J., 1994. Systematics of fluid inclusions in diagenetic minerals. SEPM Society for Sedimentary Geology.

Haas, J.L., 1971. The effect of salinity on the maximum thermal gradient of a hydrothermal system at hydrostatic pressure. Economic Geology 66, 940–946. https://doi.org/10.2113/gsecongeo.66.6.940

Hedenquist, J., 1995. The ascent of magmatic fluids: Eruption versus mineralization. pp. 263-289.

Hedenquist, J., Arribas, A., Gonzalez-Urien, E., 2000. Exploration for Epithermal Gold Deposits. Reviews in Economic Geology 13, 245–277.

Hedenquist, J., Claveria, R.J., 2001. Types of sulfide-rich epithermal deposits, and their affiliation to porphyry systems: Lepanto-Victoria-Far Southeast deposits, Philippines, as examples.

Hedenquist, J.W., Henley, R.W., 1985. The importance of CO_2 on freezing point measurements of fluid inclusions; evidence from active geothermal systems and implications for epithermal ore deposition. Economic Geology 80, 1379–1406. https://doi.org/10.2113/gsecongeo.80.5.1379

Jensen, E.P., Barton, M., 2000. Gold deposits related to alkaline magmatism. Reviews in Economic Geology 13, 279–314.

Kelley, K.D., Ludington, S., 2002. Cripple Creek and other alkaline-related gold deposits in the southern Rocky Mountains, USA: influence of regional tectonics. Min Dep 37, 38–60. https://doi.org/10.1007/s00126-001-0229-4

Lang, J.R., Stanley, C.R., Thompson, J.F.H., Pierce, F.W., Bolm, J.G., 1995. Porphyry copper-gold deposits related to alkalic igneous rocks in the Triassic-Jurassic arc terranes of British Columbia. Arizona Geological Society Digest 20, 219–236.

Liu, Y., Sun, J., Han, J., Ren, L., Gu, A., Zhao, K., Wang, C., 2019. Origin and evolution of ore-forming fluid for the Gaosongshan gold deposit, Lesser Xing'an Range: Evidence from fluid inclusions, H-O-S-Pb isotopes. Geoscience Frontiers, Groundwater Arsenic Biogeochemistry 10, 1961–1980. https://doi.org/10.1016/j.gsf.2019.01.006

Mehrabi, B., Siani, M.G., Goldfarb, R., Azizi, H., Ganerod, M., Marsh, E.E., 2016. Mineral assemblages, fluid evolution, and genesis of polymetallic epithermal veins, Glojeh district, NW Iran. Ore Geology Reviews 78, 41–57. https://doi.org/10.1016/j.oregeorev.2016.03.016

Moncada, D., Mutchler, S., Nieto, A., Reynolds, T., Rimstidt, J., Bodnar, R., 2012. Mineral Textures and Fluid Inclusion Petrography of the Epithermal Ag-Au Deposits at Guanajuato, Mexico: Application to Exploration. Journal of Geochemical Exploration 114, 20–35. https://doi.org/10.1016/j.gexplo.2011.12.001

Monger, J.W.H., 1984. Cordilleran tectonics; a Canadian perspective. Bulletin de la Société Géologique de France S7-XXVI, 255–278. https://doi.org/10.2113/gssgfbull.S7-XXVI.2.255

Nash, J.T., 1976. Fluid-Inclusion Petrology - Data from Porphyry Copper Deposits and Applications to Exploration (No. 907- D), Professional Paper. U.S. Geological Survey. https://doi.org/10.3133/pp907D

Richards, J.P., 2013. Giant ore deposits formed by optimal alignments and combinations of geological processes. Nature Geosci 6, 911–916. https://doi.org/10.1038/ngeo1920

Roedder, E., 1984. Volume 12: fluid inclusions. Reviews in mineralogy 12, 644.

Sander, M.V., Black, J.E., 1988. Crystallization and recrystallization of growth-zoned vein quartz crystals from epithermal systems; implications for fluid inclusion studies. Economic Geology 83, 1052–1060. https://doi.org/10.2113/gsecongeo.83.5.1052

Sillitoe, R., Hedenquist, J., 2003. Linkages between volcanotectonic settings, ore-fluid compositions, and epithermal precious-metal deposits, in: Society of Economic Geologists: Special Publication. pp. 315–343.

Sillitoe, R.H., 1973. The tops and bottoms of porphyry copper deposits. Economic Geology 68, 799–815. https://doi.org/10.2113/gsecongeo.68.6.799

Spooner, E.T.C., 1993. Magmatic sulphide/volatile interaction as a mechanism for producing chalcophile element enriched, Archean Au-quartz, epithermal Au-Ag and Au skarn hydrothermal ore fluids. Ore Geology Reviews 7, 359–379. https://doi.org/10.1016/0169-1368(93)90001-F

Steele-MacInnis, M., 2018. Fluid inclusions in the system H_2O-NaCl-CO_2: An algorithm to determine composition, density and isochore. Chemical Geology 498, 31–44. https://doi.org/10.1016/j.chemgeo.2018.08.022

Steele-MacInnis, M., Lecumberri-Sanchez, P., Bodnar, R., 2012. HokieFlincs_H_2O-NaCl: A Microsoft Excel spreadsheet for interpreting microthermometric data from fluid inclusions based on the PVTX properties of H_2O–NaCl. Computers & Geosciences 49, 334–337. https://doi.org/10.1016/j.cageo.2012.01.022

Thompson, J., Lang, J., Stanley, C., 2001. Platinum group elements in alkaline porphyry deposits, British Columbia. Exploration and Mining in British Columbia, Mines Branch.

Voegeli, P., 2022. Geochemistry and Mineralogy of the Silver Pond Prospect in the Toodoggone District: Implications for Regional Exploration [WWWDocument]. ERA. https://doi.org/10.7939/r3-k33m-0g39

Voegeli, P., Lecumberri-Sanchez, P., 2022. Spectral and Geochemical Characterization of the Silver Pond Argillic– Advanced Argillic Alteration Lithocap, Lawyers Property, Toodoggone District, North-Central British Columbia (Part of NTS 094E). Geoscience BC.

Wang, L., Qin, K.-Z., Song, G.-X., Li, G.-M., 2019. A review of intermediate sulfidation epithermal deposits and subclassification. Ore Geology Reviews 107, 434–456. https://doi.org/10.1016/j.oregeorev.2019.02.023

White, N.C., Hedenquist, J.W., 1995. Epithermal Gold Deposits: Styles, Characteristics and Exploration. SEG Discovery 1–13. https://doi.org/10.5382/SEGnews.1995-23.fea

Wilkinson, J.J., 2001. Fluid inclusions in hydrothermal ore deposits. Lithos, Fluid Inclusions: Phase Relationships - Methods - Applications. A Special Issue in honour of Jacques Touret 55, 229–272. https://doi.org/10.1016/S0024-4937(00)00047-5

Appendix

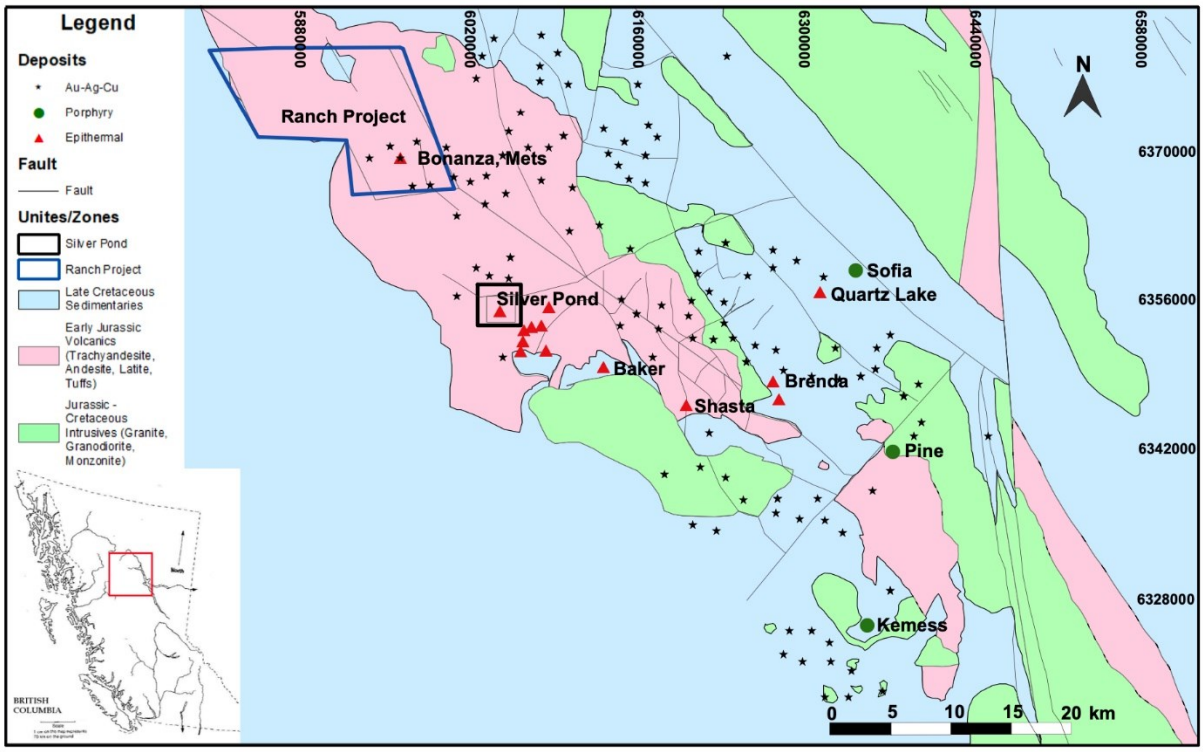

Figure 1: Regional Geological Map of Toodoggone District.

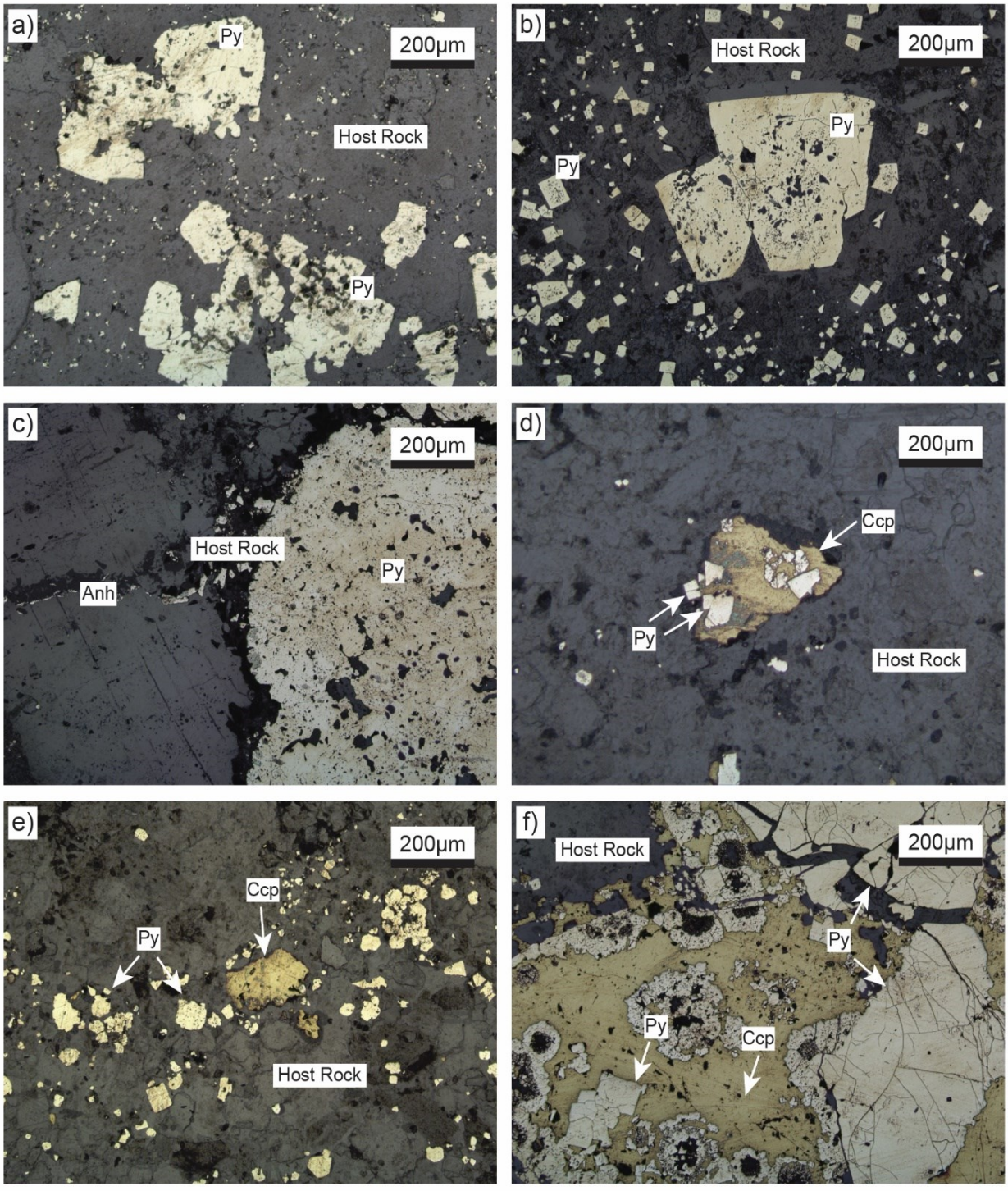

Figure 2: Disseminated Sulfide Minerals Under Reflected Light in the Silver Pond. a, b) disseminated cubic pyrites in host rock. c) rare occurrences of pyrites within anhydrite veins. d, e, f) supergene chalcopyrites on pyrites. Abbreviations: Py = pyrite; Anh = anhydrite; Ccp = chalcopyrite.

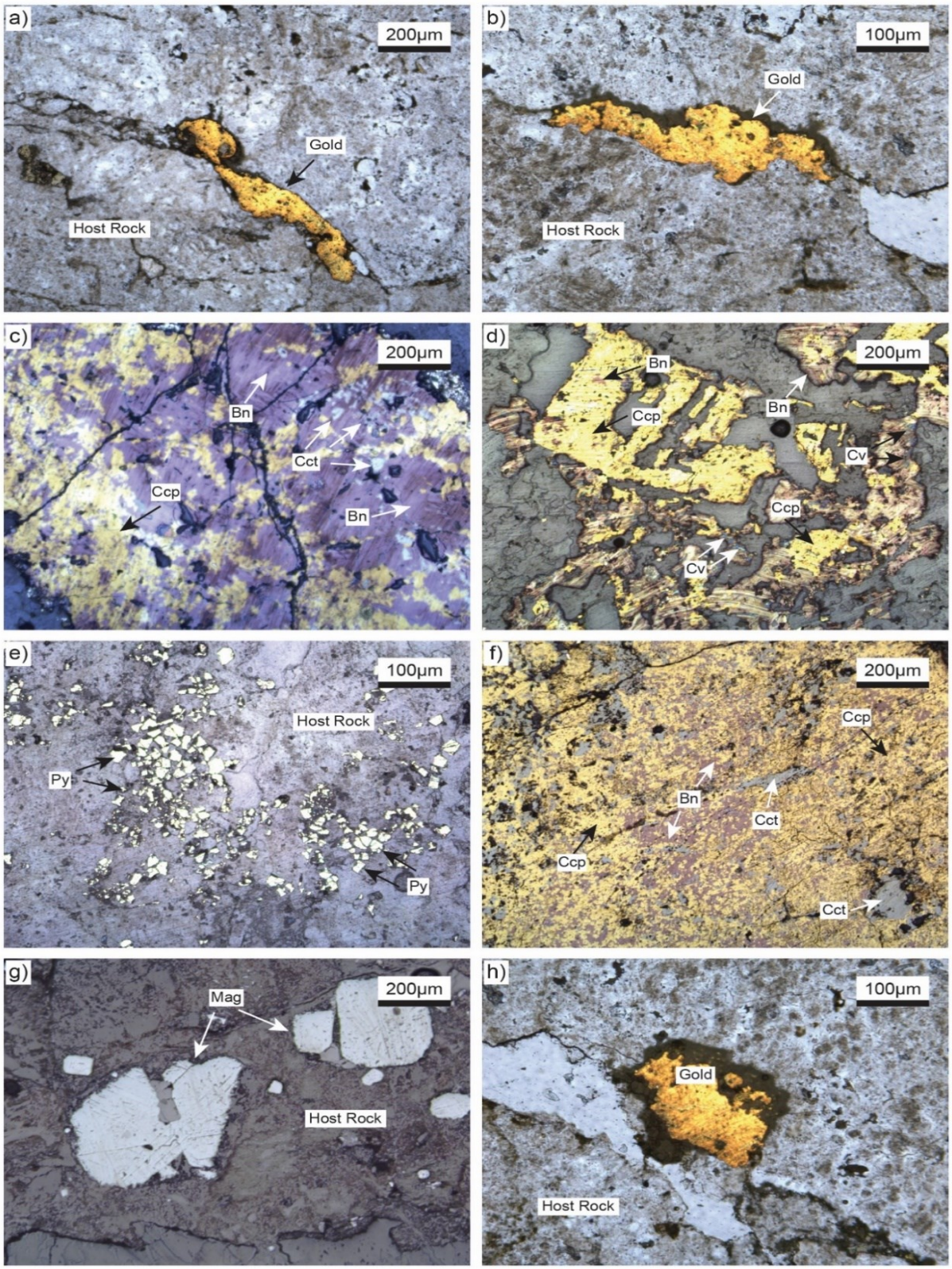

Figure 3: Ore Mineralizations with Gold grains Under Reflected Light in Ranch zones. a, b, h) disseminated gold grains in the host rock. c, d, f) supergene occurrences of Cu-sulfides (bornite, chalcocite, covellite). e) tiny cubic pyrite crystals. g) euhedral to subhedral magnetite grains in the host rock. Abbreviations: Ccp = chalcopyrite; Bn = bornite; Cct = chalcocite; Cv = covellite; Py = pyrite; Mag = magnetite.

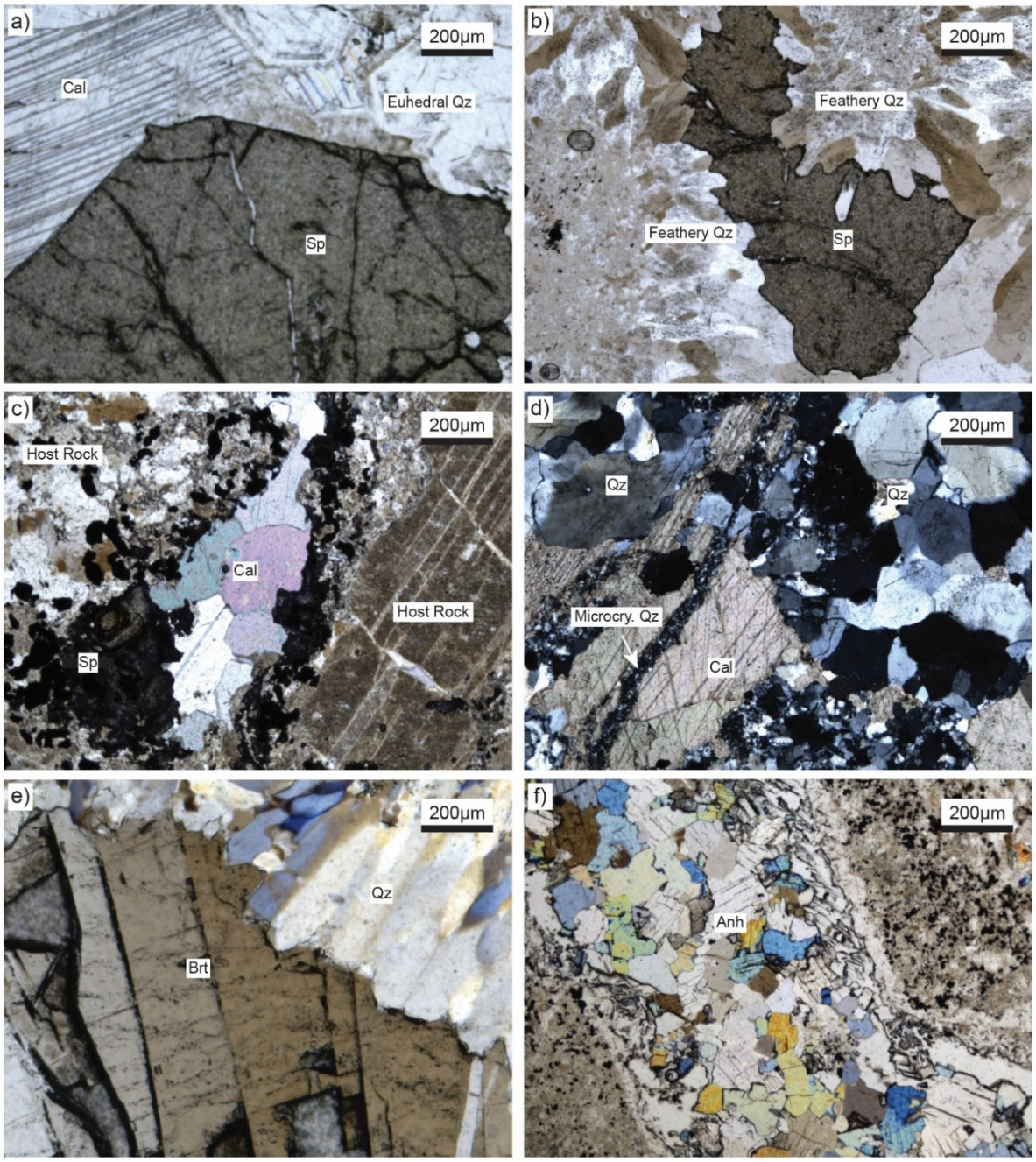

Figure 4: Gangue Mineralizations within veinlets with crosscutting relationships under Polarized Light in Silver Pond. a) euhedral quartz, calcite and sphalerite in the same vein. b) feathery quartz and sphalerite hosted vein/breccia texture. c) sphalerite and calcite bearing vein in the host rock. d) calcite crystal cut by microcrystalline quartz. e) baryte and quartz in the wall boundary. f) monomineralic anhydrite veinlet. Abbreviations: Qz = quartz; Cal = calcite; Sp = sphalerite; Microcry. Qz. = microcrystalline quartz; Brt = baryte; Anh = anhydrite.

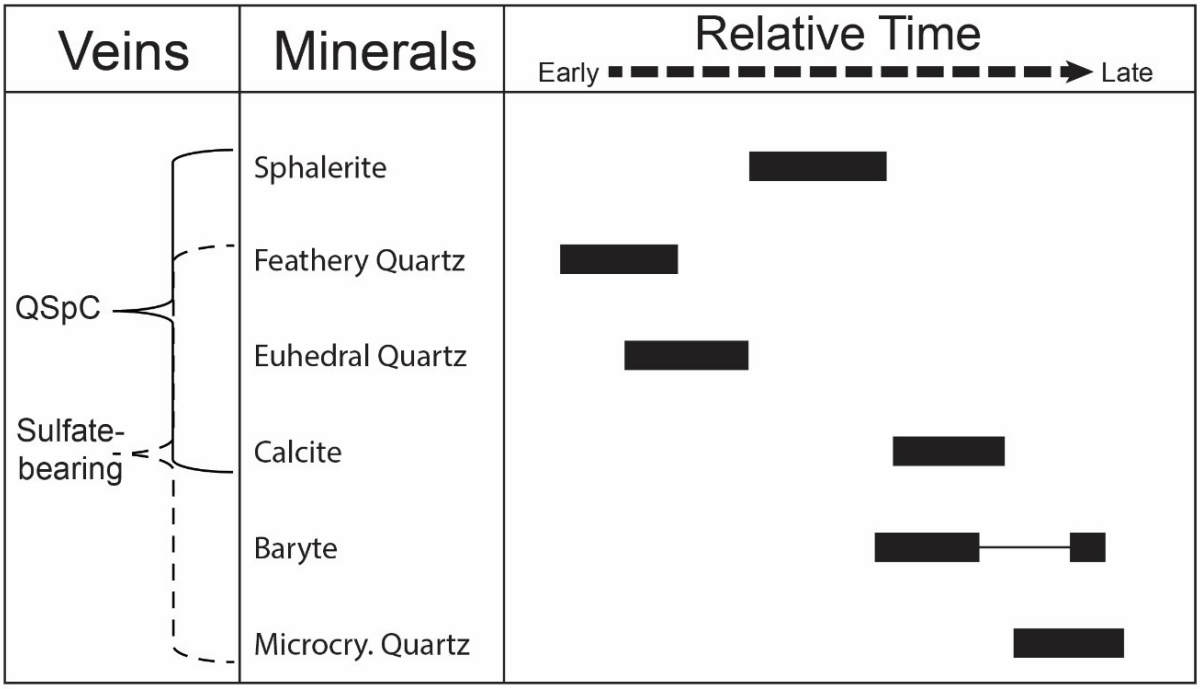

Figure 5: Relative Mineral Paragenetic Sequence in Silver Pond.

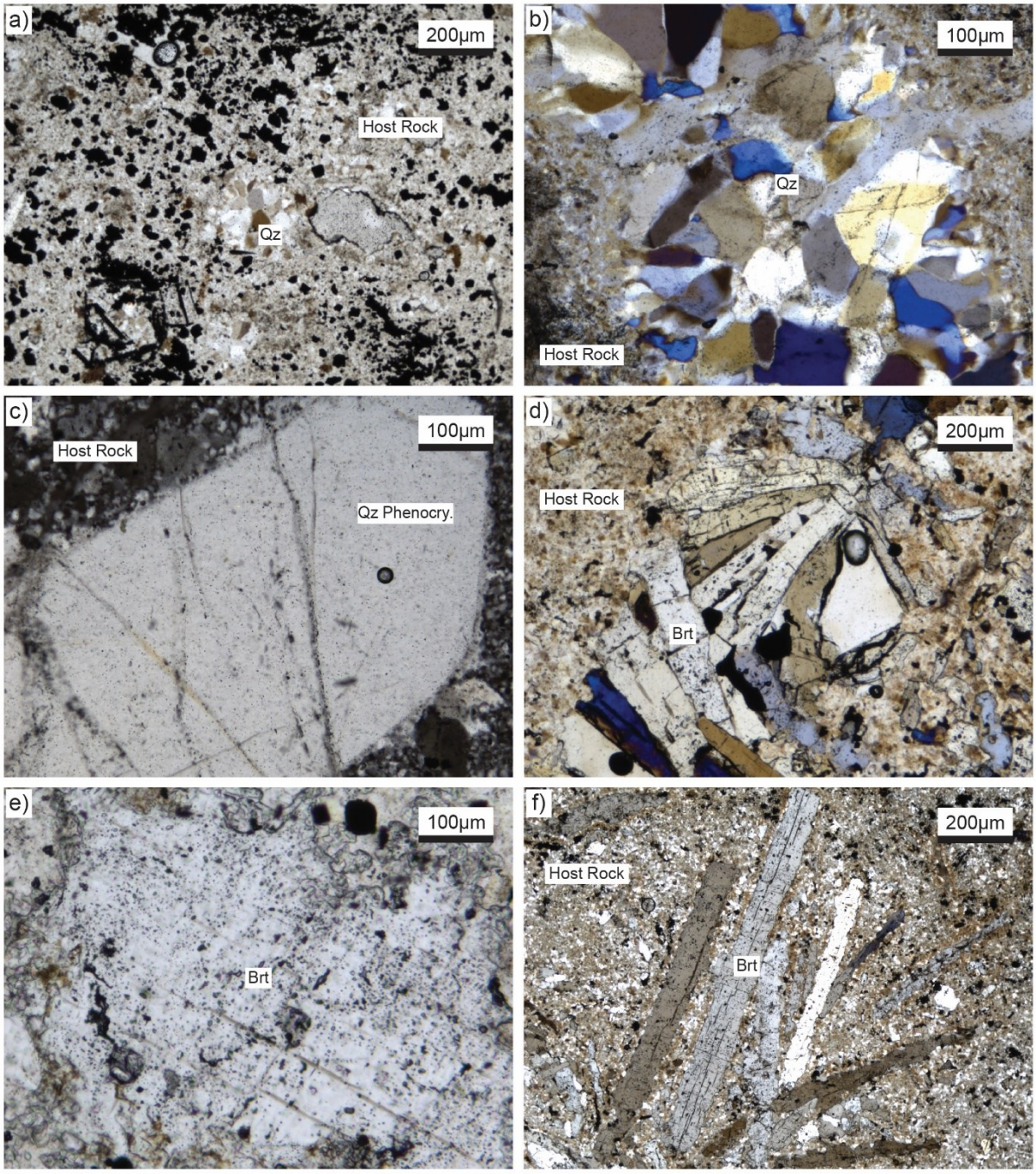

Figure 6: Gangue Mineralizations within vug fillings under Polarized Light in Ranch zones. a, b) quartz vug fillings in the host rock. c) igneous quartz phenocrystal in the volcanic host rock. d, e, f) acicular and tabular baryte crystals. Abbreviations: Qz = quartz; Qz. Phenocry. = quartz phenocrystal; Brt = baryte.

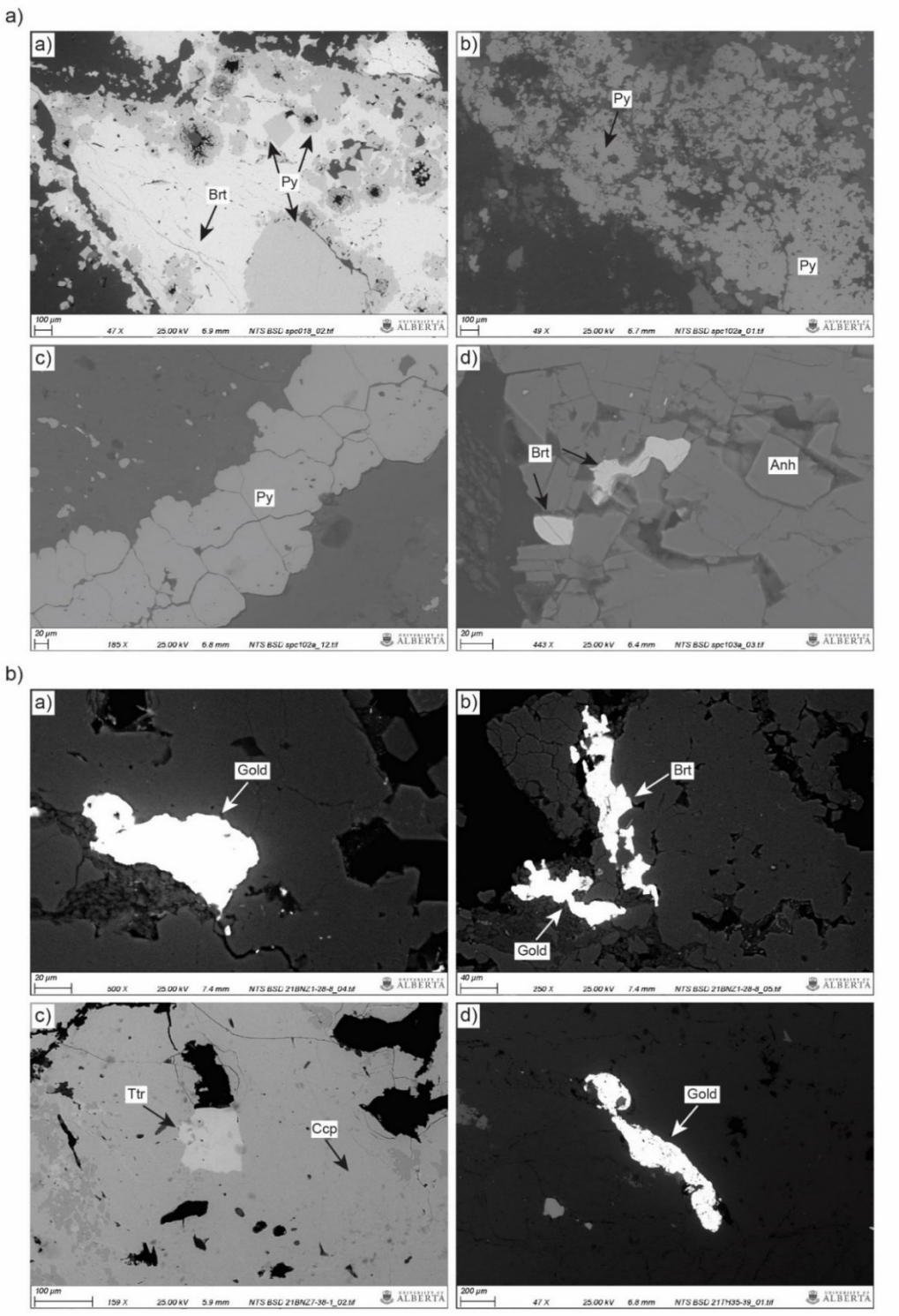

Figure 7: Backscattered Electron Imaging by Scanning Electron Microscopy. 7a) Silver Pond, 7b) Ranch zones. a-a) pyrites included within baryte grains. a-b,c) pyrites under SEM BSE imaging. a-d) barytes crystals included by anhydrite. b-a,d) gold grains in the host rock under SEM BSE imaging. b-b) gold grain and affinity with baryte under BSE imaging. b-c) chalcopyrite and Te- Bi-bearing tetrahedrite subgroup mineral under BSE imaging. Abbreviations: Py = pyrite; Brt = baryte, Anh = anhydrite; Ccp = chalcopyrite; Ttr = tetrahedrite.

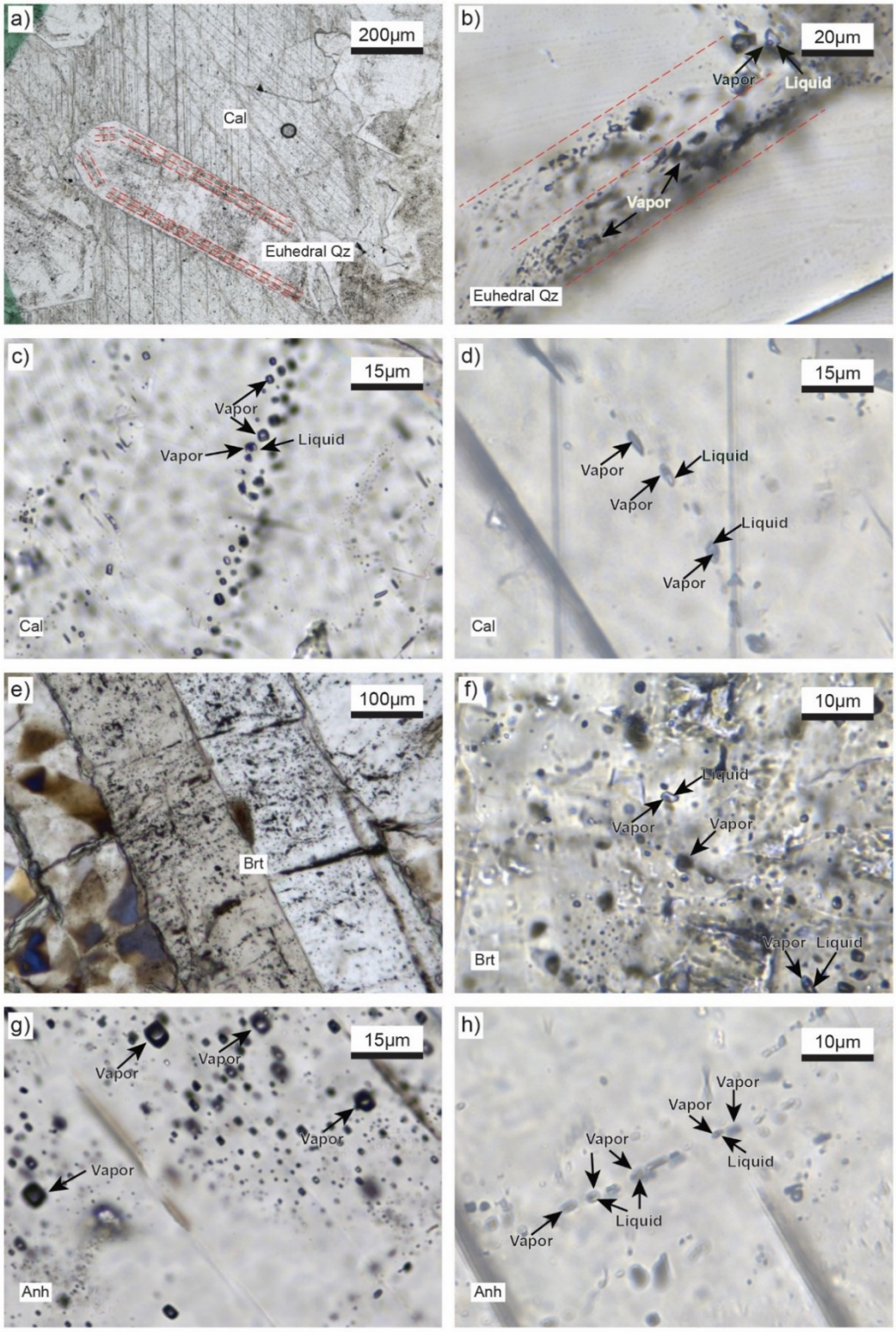

Figure 8: Fluid Inclusion Microphotographs under Polarized Light in Silver Pond. a, b) primary fluid inclusions in the euhedral quartz growth zones. c, d) secondary or uncertain origin aqueous liquid- and vapor-rich fluid inclusions in the same assemblage in calcite crystals. e, f) aqueous vapor-rich fluid inclusions in baryte. g) negative-shaped vapor inclusions in anhydrite. h) tiny aqueous liquid- and vapor-rich fluid inclusions in anhydrite. Abbreviations: Qz = quartz; Cal = calcite; Brt = baryte; Anh = anhydrite.

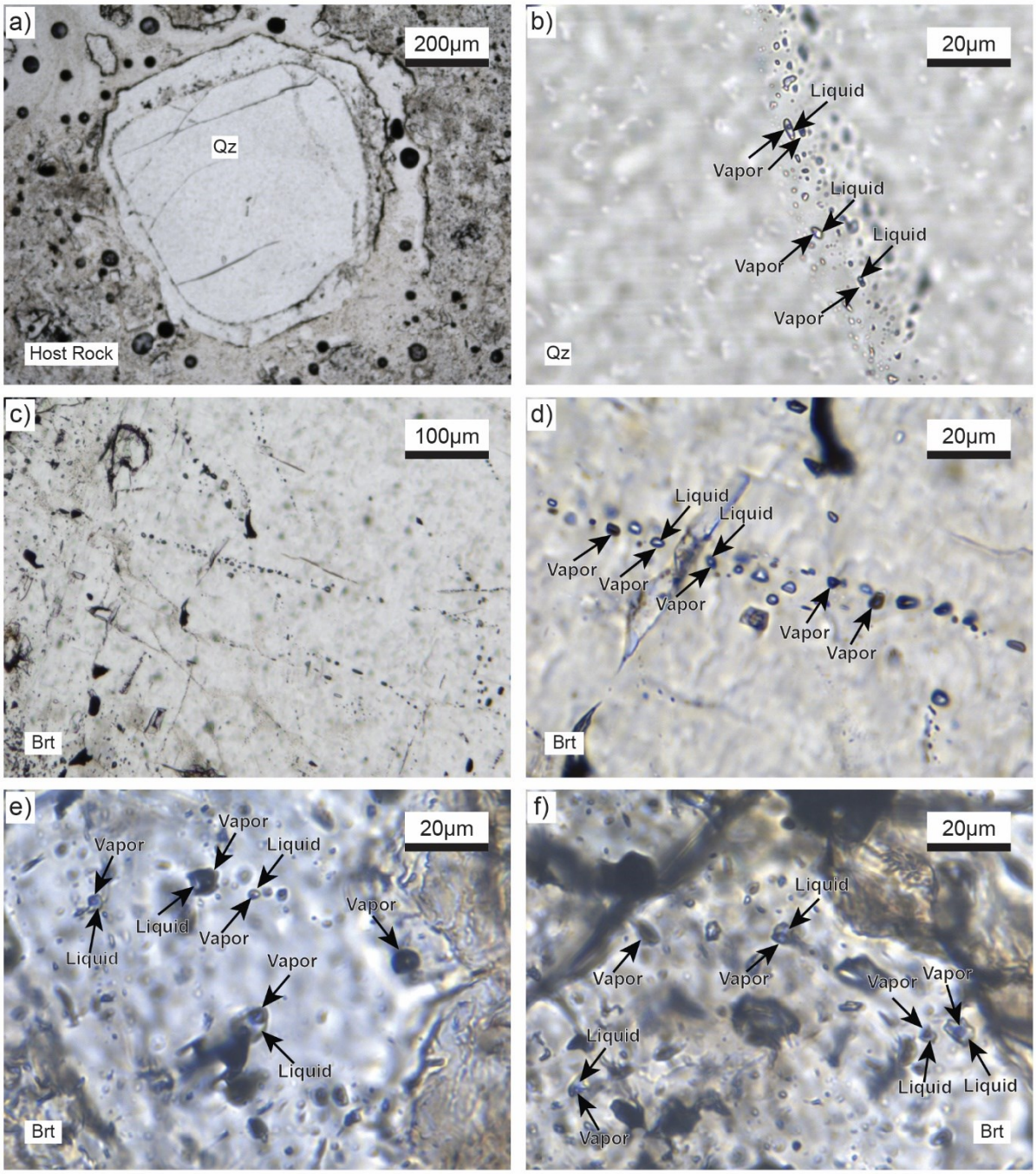

Figure 9: Fluid Inclusion Microphotographs under Polarized Light in Ranch zones. a) primary quartz phenocrystal including primary and secondary fluid inclusions. b) secondary and mainly aqueous liquid-rich fluid inclusions in primary quartz phenocrystal. c, d, e, f) uncertain origin aqueous liquid- and vapor-rich fluid inclusions in the same fluid inclusion assemblage in baryte crystal. Abbreviations: Qz = quartz; Brt = baryte.

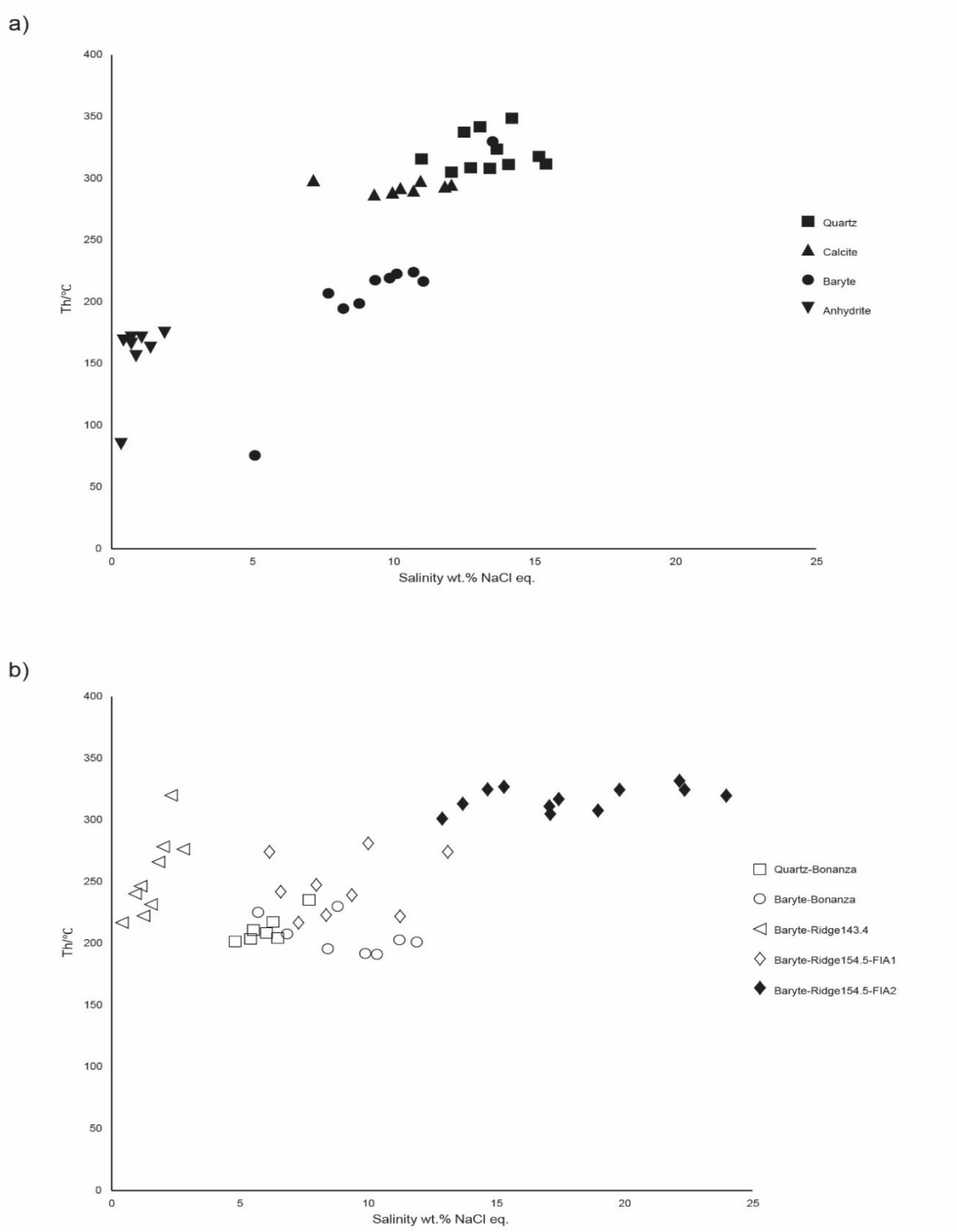

Figure 10: Microthermometry Plot Diagram – Homogenization Temperature vs. Salinity wt. % NaCl eq. 10a) Silver Pond, 10b) Ranch zones. a) decrease in salinity accompanied by decreasing Th is the main trend at Silver Pond suggesting that the hot magmatic fluid mixed with a cold, surface-derived (meteoric) water. b) the Ranch zones show similar changes in salinities within a much more limited range of homogenization temperatures, suggesting isothermal fluid mixing between a saline and a dilute fluid that were both at similar temperatures.